CATALYSIS RESEARCH

Research Article

Azadirachta *indica* Leaf Mediated Synthesis of Iron Nanoparticles and Their Catalytic Application in Methylene Blue Degradation

Ajay Rathore, Vijay Devra*

Department of Chemistry, Janki Devi Bajaj Government Girls College, Kota, Rajasthan, 324001, India

***Corresponding author:**

Vijay Devra

Department of Chemistry, Janki Devi Bajaj Government Girls College, Kota, Rajasthan, 324001, India

Email: V_devra1@rediffmail.com

Received : March 09, 2023
Published : April 04, 2023

ABSTRACT

The objective of this work was to investigate the production of iron nanoparticles (FeNPs) employing an *Azadirachta indica* leaf extract. The effects of reaction temperature and solution pH on the synthesis of iron nanoparticles were investigated. The UV-visible absorption peaks of the phyto-synthesized FeNPs were at 258 nm, and FT-IR analysis identified several functional groups that are involved in the bio-reduction of FeNPs. Iron nanoparticles were studied using SEM and TEM to define their morphology. The results show that the particles are spherical in shape and have an average size of 48 nm. Additionally, spectrophotometric analysis was used to determine the catalytic activity of the synthesized NPs on the degradation of methylene blue (MB) in the presence of Peroxodisulphate (PDS). The kinetics of MB decomposition was enhanced by Peroxodisulphate, dye, increasing concentrations of nanoparticles, and high temperatures. The maximum MB decomposition efficiency for the FeNPs/PDS system was 98% in 90 minutes under optimal reaction conditions. Thus, the current study contributes to the development of green synthesis that is affordable, reduces the use of harmful chemicals, and has diverse applications in the biological sciences.

Keywords: *Azadirachta indica*, Iron nanoparticles, catalytic activity, Methylene Blue, Peroxodisulphate

INTRODUCTION

Numerous industries release organic dyes into the environment during the manufacturing and processing of such dyes [1-3]. Methylene blue (MB) is a type of dye that is frequently used in industrial processes such as those that deal with textiles, printing, paper, pharmaceuticals, and cosmetics [4]. As a carcinogenic, poisonous, and non-biodegradable pollutant, MB poses a major risk to both human health and environmental security [5]. Additionally, the microorganisms in conventional biological treatment techniques are remarkably antibiotic-resistant to this type of pollution. It is crucial to investigate a

workable technique to reduce the damage of MB caused by water pollution.

To efficiently remove MB, several physical and chemical treatment methods, including photo-catalysis [6], adsorption [7], coagulation [8], and chemical oxidation [9], have been studied. Due to the high removal efficiency of refractory chemicals, advanced oxidation processes (AOPs) have among them demonstrated great potential in advanced treatment [10,11,12]. Due to their great efficiency and selectivity towards contaminants, sulfate radicals (SRs) ($SO_4^{\bullet-}$) based AOPs have attracted interest for their ability to degrade organic pollutants [13,14]. According to Zhang, et al. (2016), SRs have a greater redox potential than hydroxyl radicals (HO•), which range from 1.8 to 2.7 V [15]. Peroxosulphate can be activated by a variety of transition metals, including Fe(II), Co(II), Ru(III), Ce(III), Cu(II), and Ag(I) [16-20] has been widely studied. Among these transition nanometal ions, iron-mediated degradation of PDS is a powerful catalytic mechanism that produces sulfate radicals ($SO_4^{\bullet-}$) as the main oxidative product [16]. Due to its benefits, including a wide pH range, a little amount of iron catalyst, and a high degradation efficiency at room temperature, the FeNPs/PDS system for the degradation of organic contaminants has attracted a lot of attention.

Due to their eco-friendly, economical, reproducible nature, and large-scale synthesis, green and/or biosynthesis of metal nanoparticles has drawn significant attention among the synthesis methods [21]. Microorganisms, enzymes, and plants have all been reported to be used in the biosynthesis of FeNPs [22-24]. The advantage of using plant-based materials over other biological sources is that they include more potent bioactive compounds and/or secondary metabolites that can be efficiently reduced and serve as a capping agent for the production of FeNPs [25]. Bio-based nano materials has received a lot of attention in the field of nanoscience and technology due to its unique characteristics and wide variety of applications, including photocatalysis, sonocatalysis, etc., of nano-size catalysts have attracted attention in recent years to improve the performance of catalysts [26,27]. There are very few investigations where a catalyst is carried out using NPs of a certain shape and size. Various NP sizes have different active locations and surface areas. It follows that there will be variation in the catalytic activity in a particular process. As a result, achieving a regulated synthesis procedure for NPs is essential for improving catalysis [19].

This study uses leaf extract from A. indica, an Indian medicinal plant, to create FeNPs from ferrous chloride in an economical and environmentally beneficial manner (Neem). *Azadirachta indica*, a member of the Meliaceae family, is common in India and tropical Africa. It contains a variety of phytochemicals, including terpenoids, polyphenols, flavonoids, and flavanones [21,28]. Since the plant includes a range of secondary metabolites and/or bioactive compounds, it may be employed as a biological reducing agent as well as a capping agent in the synthesis of FeNPs [25]. Studies have demonstrated that the temperature of the synthesis process and the solution's pH have a significant impact on the size of FeNPs. The characteristics of produced FeNPs were determined by several instrumental methods. It has also been observed that FeNPs can remove the color from other dyes like bromothymol blue [29], Malachite green [30] and Rhodamine B [31]. Thus, the key aims of this paper are to (1) Biosynthesis of FeNPs using a simple and environmentally friendly method, without the need for any specific experimental conditions. (2) The impact of solution pH and synthesis temperature on nanoparticle formation (3) Examine the catalytic activity of synthesized NPs for the degradation of the model organic pollutant Methylene Blue in the FeNPs/PDS system (4). To ascertain the impact of various PDS, dye, catalyst, and pH concentrations on the degradation of methylene blue. The outcomes add to a better comprehension of the reaction process and mechanism of the FeNPs/PDS system.

EXPERIMENTAL

Materials and Methods

Reagent grade (AR), Methylene blue (MB), $Na_2S_2O_8$ (PDS), Ferric Chloride ($FeCl_3$), H_2SO_4, and NaOH were the chemicals used in the tests. They were all purchased from E. Merck. Fresh *Azadirachta indica* (Neem) leaves were procured from Kota, Rajasthan, India, for use in the current study (Figure 1). The collected leaves were rinsed with deionized distilled water after being washed with running tap water to remove the dust particles that were on their surface. 100 ml of distilled water and 10 gm of freshly cleaned Neem leaves were stirred at 80°C for 20 minutes on a magnetic stirrer. Filtration of the contents through Whatman filter paper and subsequent storage of the clean filtrate at 4° C for further FeNPs synthesis.

Figure 1: Photograph of Neem Leaves.

Instrumentation

To evaluate morphological characteristics, scanning electron microscopy (SEM; Nova Nano FE-SEM 450 (FEI), US) and transmission electron microscopy (TEM; Tecnai G2 20 (FEI) S-Twin, US) at 200 kV were both employed. After being centrifuged and ultrasonically dispersed for 40 minutes, dispersed NPs were mounted on a standard carbon-coated Cu grid and dried under an IR lamp for TEM analysis, and 30 L aliquots were taken and placed on the stub for SEM study. The FTIR, ALPHA-T Bruker, Germany, was used to examine the functional groups on the surface of FeNPs. For FTIR measurement, a 1% (w/w) sample was combined with 100 mg of KBr powder. The mixture was then pressed into a sheer slice. An average of 32 scans at a resolution of 4 cm^{-1} were taken for each measurement. The $FeCl_3$ solution's bio-reduction was confirmed to be complete by analysis utilizing a Peltier accessory (temperature-controlled) connected to a spectrophotometer (3000+ LAB INDIA) with a resolution of 1 nm, as well as to carry out a degradation experiment.

Iron Nanoparticles (FeNPs) Synthesis

For the synthesis, a dropwise addition of 15% leaf extracts was added to an aqueous solution containing 1.0 x 10^{-3} mol/dm^3 $FeCl_3$, which had been heated to 60°C in an oil bath with continuous magnetic stirring. UV-Visible spectra of the solution at various times and color changes allowed researchers to observe the formation of nanoparticles. According to our earlier investigation, the colloidal brownish-black color demonstrates the complete reduction of Fe^{+3} ions into Feo [25]. After 15-minute centrifugation of the resulting dispersion, the supernatant was kept at 4°C. The synthesis of FeNPs was verified using a variety of spectrophotometric methods. Additionally, the impact of varying temperatures and pH on the synthesis process was investigated.

Kinetic Measurements

In an Erlenmeyer flask set at 30°C, mix the required amount of MB, FeNPs, and other reactants as an aqueous solution. PDS aqueous solution in a known volume was used to start the reaction. The kinetics were observed by measuring the absorbance of MB spectrophotometrically at a maximum wavelength of 665 nm at regular intervals. It was observed that the dye is degrading over time, as evidenced by a decrease in the dye solution's absorbance. It was observed that there is a linear relationship between time and Log(C/C0), which supports pseudo-first-order kinetics. At least 80% of the reaction's progress is being measured.

RESULTS AND DISCUSSION

Metal nanoparticle characterization results

The analysis of metal nanoparticles using UV-Visible absorbance spectroscopy has proven to be very beneficial. The surface plasmon resonance frequency is particularly sensitive to the shape and size of nanoparticles because they have a high surface area-to-volume ratio. Figure 1 shows the UV-Visible spectra of samples that were recorded at various time intervals for color change during the synthesis of FeNPs (inset). Similar color differences have also been seen in earlier investigations [32]. After 60 minutes, dark brown color and a strong SPR peak with maximum absorption at 258 nm appeared, demonstrating the synthesis of FeNPs (Figure 2) [33]. Furthermore, the slight increase in absorbance leads the light brown color to change to dark brown, indicating the development of a nanocluster of zero-valent FeNPs.

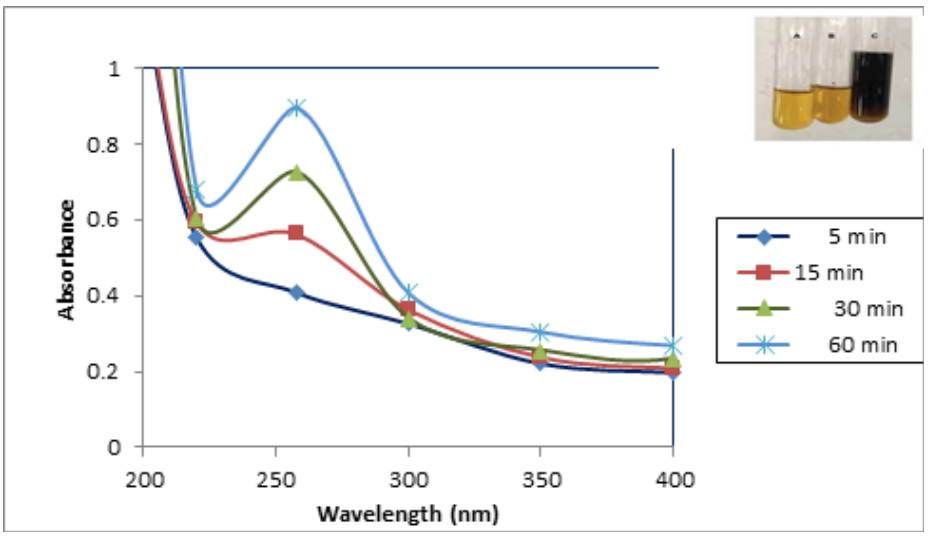

Figure 2: The color change of the dispersion photographs and the UV-Visible absorption spectra of FeNPs.

As shown in figure 3, the particle shape of the synthesized FeNPs, as confirmed by TEM investigation, is spherical, with an average size of 48 nm. SEM scans show that the nanoparticles have been produced with well-defined morphology and are nearly spherical [34]. In the TEM image, FeNPs are separated from one another, demonstrating efficient capping by water-soluble biomolecules found in the A. Indica leaves extract. It is known that when biomolecules connect to the surface of FeNPs, their surface charge increases noticeably and their stability is improved by preventing aggregation [35].

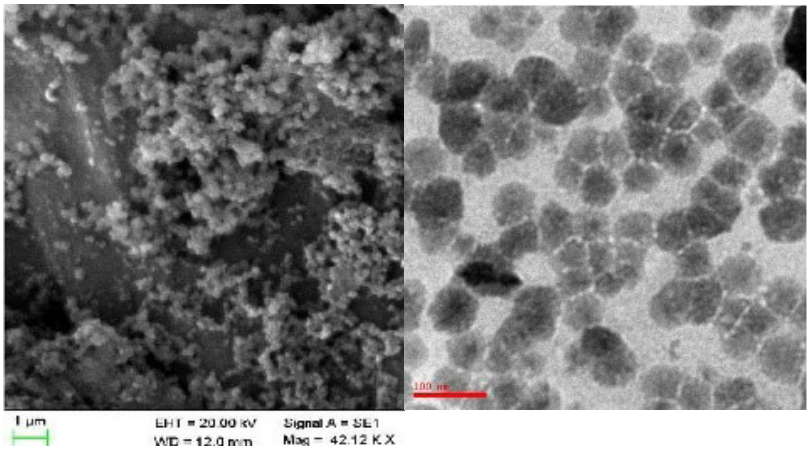

Figure 3: [a] SEM image [b] TEM image of synthesized FeNPs at optimum reaction condition ($FeCl_3$ =1.0 x10^{-3} mol / dm3, leaf Extract= 15% pH=6.0 and Temp=60°C).

The FTIR examination of the produced nanoparticles, shown in Figure 4, indicated that these FeNPs are stable for one month at 4°C due to the bio capping of neem leaf extract. The major peak of synthesized FeNPs is at 3393.36 cm^{-1}; significant absorption suggested the presence of alcohols and phenols as well as OH stretching vibrations [36]. The peaks at 2922.10 and 2352.02 cm–indicates the C-H stretching vibrations of alkanes and –OH stretching of amino acids. The O–H stretch in the nanoparticles is due to the secondary metabolites such as polyphenols, sugars, and amino acids which have been reported to be responsible for chelation and bio-reduction of Fe^{3+} and Fe^{2+} to Feo [37]. These also explain their roles as capping agents as they are also observed in spectra of iron nanoparticles.

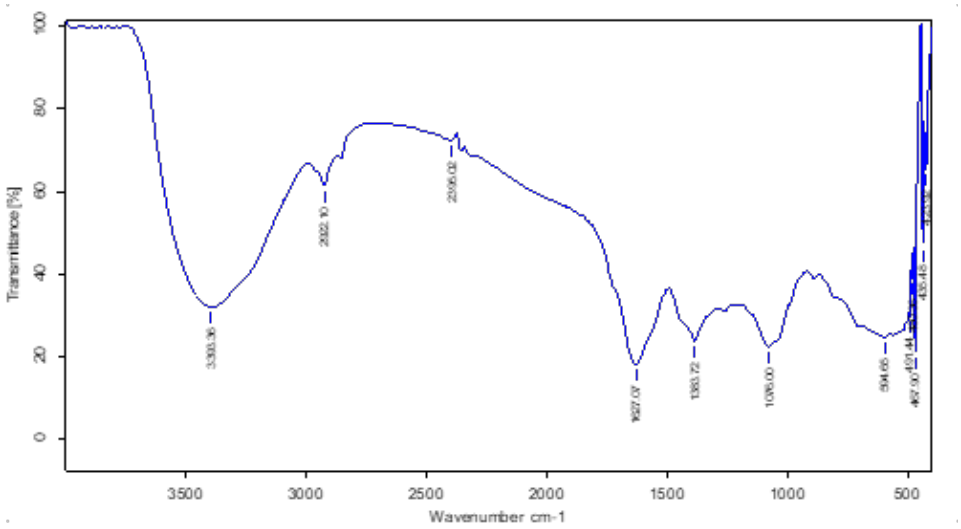

Figure 4: FT-IR Spectra of green synthesized FeNPs.

The current study also examined how temperature affected the production of nanoparticles at three distinct temperatures, 50°, 60°, and 70°C, respectively. The nanoparticles were agglomerated at higher temperatures (70°C), but they are well disseminated and have an average size of around 48 nm at 60°C, as shown in Fig. 5. Raising the reaction temperature accelerated the reduction of Fe^{+3}. As a result, the synthesis rate is too high at high temperatures to control particle size. According to Harshiny, et al. [33], increasing the reaction temperature led to an increase in the rate of reduction of iron nanoparticles. Additionally, SEM findings (Figure 6) support it. Therefore, iron nanoparticles should be created at a moderate temperature (60°C) with proper size control.

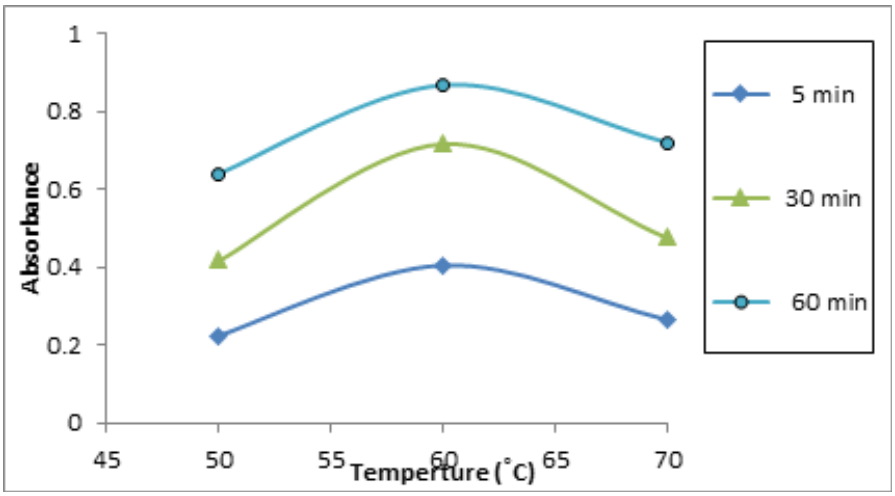

Figure 5: Time course of iron nanoparticles synthesis with different reaction temperatures (50- 70°C), $FeCl_3$ (1.0×10^{-3} mol /dm^3), leaf extract= 15% pH=6.0.

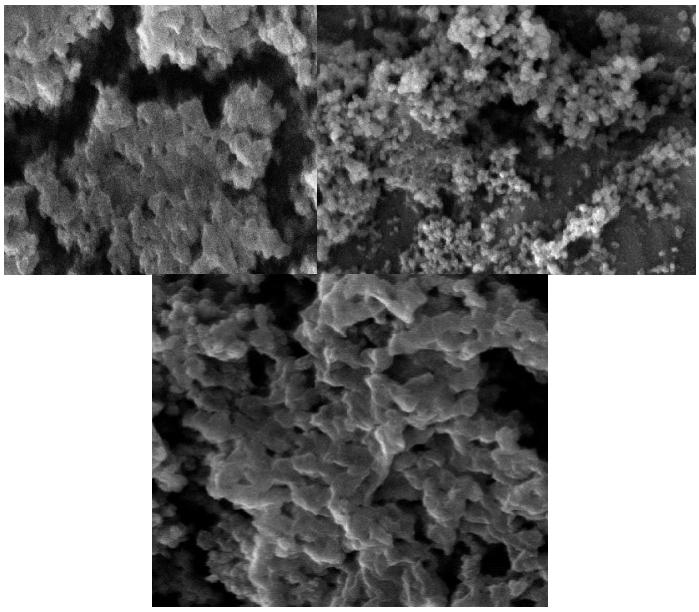

Figure 6: SEM image of Synthesized FeNPs at the different Temperatures(A) 500 (B) 600, and (C) 700C.

The solution pH was one of the key factors for the synthesis of nanoparticles, and the rate of synthesis and morphology of NPs are affected by pH variations [21]. Figure 7 illustrates the absorbance spectra used to examine the impact of solution pH on the formation of NPs. Due to the presence of unreacted organic molecules in the reaction solution at pH 4, which is acidic, the spectrum peak at 258 nm is occupied by fewer particles. The high absorbance at a pH of 6, which is nearly neutral, was caused by the activation of phytochemicals in the leaf extract. However, the absorbance peak changed at a higher pH of 10, which might be an aggregation of nanoparticles. As a finding, at 1 mM $FeCl_3$, 15% leaf extract, and 60°C temperature, the pH of 6.0 is suitable to produce FeNPs. Due to the species of leaf extract's release of H+ ions during oxidation in the presence of Fe^{3+} ions, the pH of the medium decreases during the synthesis process. [33].

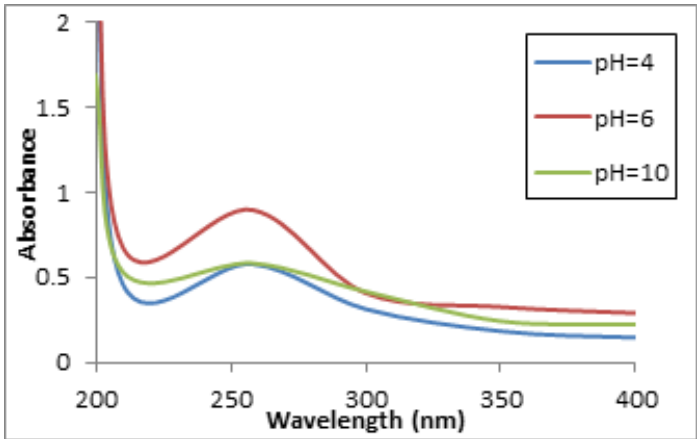

Figure 7: UV spectra recorded as a function of reaction at different wavelengths versus absorbance during synthesis of iron nanoparticles at different solution pH (4, 6, and 10).

Effect of Experimental Conditions on the Degradation Process

UV-visible spectra of intermediates and degradation pathway

Figure 8. depicts the temporal evolution of the UV–vis spectra in the range of 200–800 nm of aqueous MB solution in the presence of PDS and FeNPs as a catalyst. Two main absorbance peaks are observed. Two peaks cantered at 246 nm and 292 nm in the ultraviolet region are assigned to the benzene-like structures [38]. The band comprising peaks at 614 nm and 665

nm in the visible region are chromophores made up of two aromatic rings [39]. The absorption peak at 614 nm and 665 nm is attributed to the chromophore's functional groups of MB and its dimers, namely -C=S and -C=N, which may undergo hemolytic cleavage and change into colourless substances successively. The spectra indicate these absorption peaks rapidly decrease with an increase in reaction time and almost disappear at the end of 60 min of reaction time.

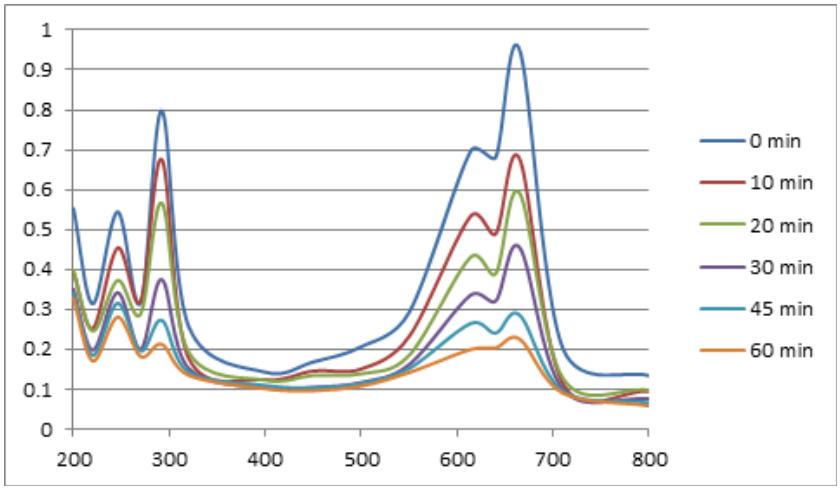

Figure 8: In the FeNPs/PDS system, the UV–vis spectrum shifts with reaction time.

([PDS] = 5 x 10^{-4} mol /dm^3, [MB] =5x10^{-5} mol /dm^3, [FeNPs] =5x10^{-8} mol /dm^3, pH=3.0 and Temperature 30°C).

The following path is proposed based on observed results obtained from spectrum changes during MG degradation (figure. 9). Initially, the $SO_4^{\cdot-}$ preferentially attacks the chromophore centre of the dye molecule, with the demethylation cleavage and release of one or more of the methyl group substituents on the amine groups, leading to the formation of azure A(m/z = 256), B (m/z = 270), and C (m/z = 241). Some middle products were produced by the destruction of benzene rings during the catalytic reaction. Finally, the breakdown of aromatic rings takes place and the resultant smaller intermediates subsequently undergo successive degradation reactions to yield carbon dioxide and water. Therefore, catalysis using FeNPs/PDS system is a green and effective method to purify methylene blue.

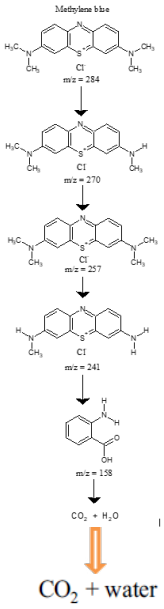

Figure 9: Proposed Degradation pathway of MB by PDS-FeNPs system.

Effect of Experimental Condition

Peroxodisulphate dependence

PDS is a major source of Sulfate radicals in the FeNPs/PDS system and was examined at different PDS concentrations ranging from 1.0 x 10^{-4} to 1.0 x 10^{-3} mol/dm^3 at 30^{oC} temperature, with constant concentrations of MB at 5 x 10^{-5} mol/dm^3, [FeNPs] at 5 x 10^{-8} mol/dm^3, and pH at 3.0. Due to the significant quantity of Sulfate radicals that are created at greater PDS concentrations, the rate of dye degradation increases as the initial concentration of PDS rises. Since increasing the PDS concentration above 5x10-4 mol/dm3 did not improve the effectiveness of degradation, and further likely because too much PDS would react with the side reaction between the persulfate ion $S_2O_8^{-2}$ and Sulfate radical (SO4•-) [40]. This illustrates that, at low PDS concentrations, the availability of PDS is the limiting factor determining the formation of radicals, and that, when PDS concentrations rise 5x10^{-4} mol/dm^3, the PDS contribution becomes noticeably less significant. For subsequent studies, a PDS concentration of 5x10^{-4} mol/dm^3 is selected. (Table 1)

$$S_2O_8^{-2} + SO_4^{\bullet-} \longrightarrow S_2O_8^{-} + SO_4^{-2}$$

Dye dependence

At 30°C, the initial concentration of MB varied between 1.0 x10-5 and 1.0 x10-4 mol/dm^3, whereas the concentrations of the other reactants and reaction conditions remained constant. It was determined that as the amount of MB in the FeNPs/PDS system increased, the rate of degradation increased as well. This might be explained by an increase in dye concentration, which sped up the reaction because there were more dye molecules available to degrade. After reaching a specific dye concentration (5 x 10^{-5} mol/dm^3), the degradation rate decreased (Table 1). This can be explained by the fact that there is significantly less MB decomposition when the supply of SO4$^{\bullet-}$ radicals is reduced at fixed oxidant concentration. [41].

Effect of initial pH

The performance of degradation is significantly and highly affected by pH. Experiments with various initial pH values (3, 5, 7, 9, and 11) were adjusted using either 0.1 mol/dm^3 HCl or 0.1 mol/dm^3 NaOH to evaluate the impact of the initial pH. The results demonstrate that the rate of degradation is increased at acidic pH (Table-1). Similar patterns were seen in a prior study that used nano valent iron to decompose azo dyes [42]. FeNPs/PDS system, the reaction between PDS and FeNPs was an acid-production process, which was advantageous for the oxidation reaction. The kobs at initial pH 3 (7.9x10^{-4} Sec-1) were greater than 10 times that at pH 11 (0.65x10^{-4}Sec-1). The findings demonstrated that PDS can be rapidly activated under acidic conditions to produce a potent $SO_4^{\bullet-}$(Free radical), however, PDS and SO_4^{-2} were removed under alkaline conditions. FeNPs can transfer electrons to more ions, turning them into atoms, at lower pH, where there are more H+ ions. The dye molecule is then attacked by these atoms, and it eventually degraded.

Effect of the Reaction Temperature on the Catalytic Performance

The catalytic activity of the produced FeNPs was evaluated in the oxidative degradation of MB by PDS at concentrations ranging from 1 x 10^{-8} to 10 x 10^{-8} mol dm^{-3} at constant [PDS] = 5 x 10^{-4} mol dm^{-3} [MB] = 5 x 10^{-5} mol dm^{-3}, pH = 3.0. The results exhibited that raising the temperature has a favourable impact on MB degradation (Table 1). At [FeNPs]=5x10^{-8} mol dm^{-3}, the kobs increased from 6.2 x 10^{-4} sec-1 to 8.8 x 10^{-4} sec-1 when the reaction temperature was raised from 25°C to 35°C. Furthermore, study the MB degradation by PDS without FeNPs at the same temperatures, a set of control experiments was also carried out. The degradation rate is seven times higher in the presence of a low concentration (5x10^{-8} mol dm^{-3}) of FeNPs than it is in the absence of FeNPs. (Figure 10). According to the MB degradation in these two systems, the reaction temperature considerably enhanced SO4$^{\bullet-}$ formation catalysed by FeNPs [17].

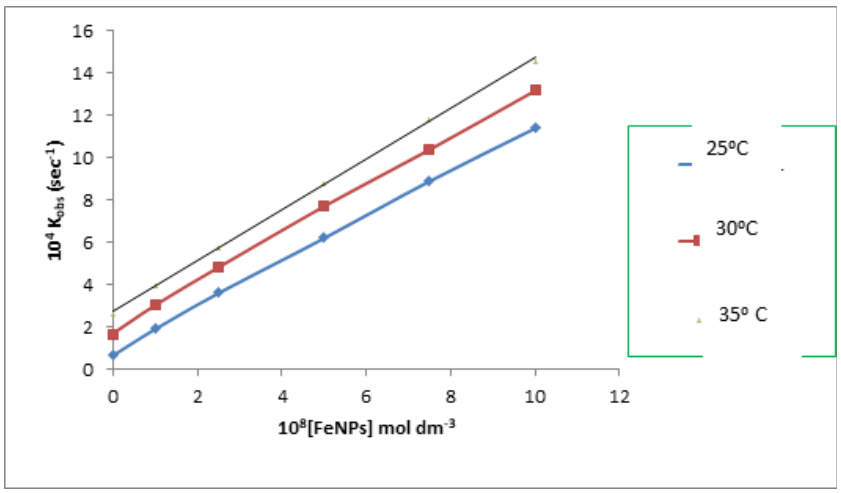

Figure 10: Effect of [FeNPs] on degradation rate of MB at three Temperature and Fixed {PDS] = 5 × 10^{-4} mol dm^{-3}[MB] = 5 x 10^{-5} mol dm^{-3} and pH= 3.0.

Table 1: Effect of variation of [PDS] [MB] [FeNPs] and pH an oxidative degradation of Methylene Blue at 30°C

S.no.	10^4[PDS] mol dm^{-3}	10^4 [MB] mol dm^{-3}	10^8[FeNPs] mol dm^{-3}	pH	10^4 Kobs (sec^{-1})
1	1.0	5.0	5.0	3.0	0.9
2	2.5	5.0	5.0	3.0	3.5
3	5.0	5.0	5.0	3.0	7.9
4	7.5	5.0	5.0	3.0	7.6
5	10.0	5.0	5.0	3.0	7.4
6	5.0	1.0	5.0	3.0	2.9
7	5.0	2.5	5.0	3.0	5.8
8	5.0	5.0	5.0	3.0	7.9
9	5.0	7.5	5.0	3.0	7.5
10	5.0	10.0	5.0	3.0	7.0
11	5.0	5.0	0.0	3.0	1.65
12	5.0	5.0	1.0	3.0	3.0
13	5.0	5.0	2.5	3.0	4.8
14	5.0	5.0	5.0	3.0	7.7
15	5.0	5.0	7.5	3.0	10.4
16	5.0	5.0	10.0	3.0	13.2
17	5.0	5.0	5.0	3.0	7.9
18	5.0	5.0	5.0	5.0	4.6
19	5.0	5.0	5.0	7.0	3.1
20	5.0	5.0	5.0	9.0	1.5
21	5.0	5.0	5.0	11.0	0.65

CONCLUSION

The biogenesis of iron nanoparticles can be carried out using aqueous extracts of *Azadirachta indica* leaves. The synthesized particles functional group analysis and characterization results showed that they were primarily made of iron with bio-functional groups. the use of the generated nanoparticles as a catalyst for the degradation of methylene blue. According to this study, the FeNPs/PDS system is an efficient oxidation method for the degradation of MB. In addition, the concentrations of the dye and PDS as well as the initial pH and reaction temperature influenced the reactivity of FeNPs/PDS. As an outcome of the research, it was concluded that silver nanoparticles had a significant amount of potential for rapid dye degradation technologies. Therefore, in brief, the major benefit of FeNPs/PDS are stronger acid-producing capacity that prevents the catalyst from passivating. Further research

on the production of other metallic nanoparticles using extracts of *Azadirachta indica* leaves is possible, and the study of the decolorization of other hazardous compounds and dyes can also be done using these bio-produced FeNPs.

REFERENCES

1. Reddy MCS, Sivaramakrishna L, Reddy AV. (2012). The use of an agricultural waste material, Jujuba seeds for the removal of anionic dye (Congo red) from aqueous medium. J Hazard Mater. 203:118–127.

2. Bhatt AS, Sakaria PL,Vasudeva M, Pawar RR, Sudheesh N, Bajaj HC, et al. (2012). Adsorption of an anionic dye from aqueous medium by organoclays: Equilibrium modeling, kinetic and thermodynamic exploration. RSC Adv. 2:8663–8671.

3. Krishna LS, Reddy AS, Muralikrishna A, Zuhairi WW,Osman H,Reddy AV. (2015). Utilization of the agricultural waste (Cicer arientinum Linn fruit shell biomass) as biosorbent for decolorization of Congo red. Desal Water Treat. 56:2181–2192.

4. Lakkaboyana SK,Khantong S, Asmel N.K, Yuzir A, Yaacob WZW. (2019). Synthesis of copper oxide nanowires-activated carbon (AC@CuO-NWs) and applied for removal methylene blue from aqueous solution: Kinetics, isotherms, and thermodynamics. J Inorg Organomet. 29:1–11.

5. Pan XH, Cheng SY, Su T, Zuo GC, Zhao W, Qi XL, et al.(2019). Fenton-like catalyst Fe_3O_4@polydopamine-MnO2 for enhancing removal of methylene blue in wastewater. Colloid Surface. 181:226–233.

6. Abdelrahman EA, Hegazey RM, Kotp YH, Alharbi A. (2019). Facile synthesis of Fe_2O_3 nanoparticles from Egyptian insecticide cans for efficient photocatalytic degradation of methylene blue and crystal violet dyes. Spectrochim Acta Part A Mol Biomol Spectrosc. 222:117195.

7. Mei S Gu, J Ma T, Li X, Hu Y, Li W, Zhang J, et al. (2019). N-doped activated carbon from used dyeing wastewater adsorbent as a metal-free catalyst for acetylene hydrochlorination. Chem Eng J. 371:118–129.

8. Zazou H, Afanga H, Akhouairi S, Ouchtak H, Addi AA, Akbour RA, et al. (2019). Treatment of textile industry wastewater by electrocoagulation coupled with electrochemical advanced oxidation process. J. Water Process. Eng. 28:214–221.

9. Pang JB, Fu FL, Li WB, Zhu LJ, Tang B. (2019). Fe-Mn binary oxide decorated diatomite for rapid decolorization of methylene blue with H_2O_2. Appl Surf Sci. 478:54–61.

10. Balcioglu IA, Otker M. (2003). Treatment of pharmaceutical wastewater containing antibiotics by O_3 and O_3/H_2O_2 processes. Chemosphere. 50:85–95.

11. Anotai J, Su CC, Tsai YC, Lu MC. (2011). Comparison of aniline oxidation by electro-Fenton and fluidized-bed Fenton processes. J Environ Eng. 137:363–370.

12. Masomboon N, Ratanatamskul C, Lu MC. (2009). Chemical oxidation of 2,6-dimethylaniline in the Fenton process. Environ Sci Technol. 43:8629–8634.

13. Silva LL, Moreira CG, Curzio BA, da Fonseca FV. (2017). Micropollutant removal from water by membrane and advanced oxidation processes-a review. J Water Resource Prot. 9(5):411-431.

14. KN R, Shrihari S, Thalla AK. (2021). Removal of micro-pollutants using green synthesized nano irpn particles by the Advanced Oxidation process. Poll Res. 40 (3):884-892.

15. Zhang J, Chen M, Zhu L. (2016). Activation of peroxomonosulphate by iron-based catalysts for orange G degradation: role of hydroxylamine. RSC Adv. 6: 47562-47569.

16. Lu J, Zhou Y, Lei J, Ao Z, Zhou Y. (2020). Fe_3O_4/graphene aerogels: A stable and efficient persulfate activator for the rapid degradation of malachite green. Chemosphere. 251:126402.

17. Nguyen TB, Doong RA, Huang CP, Chen CW, Dong CD. (2019). Activation of persulfate by CoO nanoparticles loaded on 3D mesoporous carbon nitride (CoO@ meso-CN) for the degradation of methylene blue (MB). Sci Total Environ. 675: 531-541.

18. Anipsitakis GP, Dionysiou DD. (2004). Radical generation by the interaction of transition metals with common oxidants. Environ Sci Technol. 38: 3705–3712

19. Nagar N, Devra V. (2018). Oxidative degradation of Orange G by peroxomonosulfate in presence of biosynthesized copper nanoparticles-a kinetic study. Environ Technol Innov. 10:281-289.

20. Nagar N, Devra V. (2019). A kinetic study on the degradation and biodegradability of silver nanoparticles catalyzed Methyl Orange and textile effluents. Heliyon. 5(3):e01356.

21. Nagar N, Devra V. (2018).Green synthesis and characterization of copper nanoparticles using *Azadirachta indica* leaves. Mater. Chem. Phys. 213: 44-51.

22. Vitta Y, Figueroa M, Calderon M, Ciangherotti C. (2020). Synthesis of iron nanoparticles from aqueous extract of Eucalyptus robusta Sm and evaluation of antioxidant and antimicrobial activity. Materials science for energy technologies. 3:97-103.

23. Devra V. (2022). Synthesis of metal nanoparticles by microbes and biocompatible green reagents. In Agri-Waste and Microbes for Production of Sustainable Nanomaterials. 17-45.Elsevier.

24. Devra V. (2022). Plant and agri-waste-mediated synthesis of metal nanoparticles. In Agri-Waste and Microbes for Production of Sustainable Nanomaterials. 47-77.

25. Rathore A, Devra V. (2022). Experimental Investigation on Green Synthesis of FeNPs using *Azadirachta indica* Leaves. J Sci Res. 14(1):375-386.

26. Mubeen I, Farrukh MA. (2021). Mechanisms of green synthesis of iron nanoparticles using Trifolium alexandrinum extract and degradation of methylene blue. Inorg Nano-Met Che. 9:1-10.

27. Taufik A, Tju H, Saleh R. (2016). Comparison of catalytic activities for sonocatalytic, photocatalytic and sonophotocatalytic degradation of methylene blue in the presence of magnetic Fe_3O_4/CuO/ZnO nanocomposites. In J Phys. 710:012004.

28. Rao TS, Murugan S. (2023). Experimental investigation of drying neem (*Azadirachta indica*) in an evacuated tube solar dryer: Performance, drying kinetics and characterization. Solar Energy. 253:270-284.

29. Xin H, Yang X, Liu X, Tang X, Weng L, Han Y. (2016). Biosynthesis of iron nanoparticles using tie guanyin tea extract for degradation of bromothymol blue. J Nanotechno. 27:2016.

30. Rathore A, Devra V. Single-Step Green Synthesis of Iron Nanoparticles in the Aqueous Phase for Catalytic Application in Degradation of Malachite Green. Adv. Energy Mater. 2022:16-29.

31. Xiao C, Li H, Zhao Y, Zhang X, Wang X. (2020). Green synthesis of iron nanoparticle by tea extract (polyphenols) and its selective removal of cationic dyes. J Environ Mang. 275:111262.

32. Devatha CP, Thalla AK, Katte SY. (2016). Green synthesis of iron nanoparticles using different leaf extracts for treatment of domestic waste water. J Cleaner Prod. 139:1425-1435.

33. Harshiny M, Iswarya CN, Matheswaran M. (2015). Biogenic synthesis of iron nanoparticles using Amaranthus dubius leaf extract as a reducing agent. Powder Technol. 286:744-749.

34. Karthikeyan C, Ranjani M, Kim AR, Yoo DJ. (2016). Synthesis of iron nanoparticles using *Azadirachta indica* extract and its catalytic activity toward nitrophenol reduction. J Nanosci Nanotech. 16(3):2527-2533.

35. Veeramanikandan V, Madhu GC, Pavithra V, Jaianand K, Balaji P. (2017). Green synthesis, characterization of iron oxide nanoparticles using Leucas aspera leaf extract and evaluation of antibacterial and antioxidant studies. Int J Agric Innov Res. 6(2):242-250.

36. Dharshini RS, Poonkothai M, Srinivasan P, Mythili R, Syed A, Elgorban AM, et al. (2021). Nano-decolorization of methylene blue by Phyllanthus reticulatus iron nanoparticles: an eco-friendly synthesis and its antimicrobial, phytotoxicity study. App Nanosci. 31:1-1.

37. Izadiyan Z, Shameli K, Miyake M, Hara H, Mohamad SE, Kalantari K, et al. (2020). Cytotoxicity assay of plant-mediated synthesized iron oxide nanoparticles using Juglans regia green husk extract. Arab J Chem. 13(1):2011-2023.

38. Wang X, Wang A, Ma J, Fu M. (2017). Facile green synthesis of functional nanoscale zero-valent iron and studies of its activity toward ultrasound-enhanced decolorization of cationic dyes. Chemosphere. 166:80-88.

39. Zhou G, Chen Z, Fang F, He Y, Sun H, Shi H. (2015). Fenton-like degradation of Methylene Blue using paper mill sludge-derived magnetically separable heterogeneous catalyst: Characterization and mechanism. J Environ Sci. 35: 20-26.

40. Chi H, Wan J, Ma Y, Wang Y, Ding S, Li X. (2019). Ferrous metal-organic frameworks with stronger coordinatively unsaturated metal sites for persulfate activation to effectively degrade dibutyl phthalate in wastewater. J Hazar Mater. 377:163-171.

41. Nagar N, Devra V. (2017). Activation of peroxodisulfate and peroxomonosulfate by green synthesized copper nanoparticles for Methyl Orange degradation: a kinetic study. J Environ Chem Eng. 5(6):5793-5800.

42. Lu J, Zhou Y, Lei J, Ao Z, Zhou Y. (2020). Fe3O4/graphene aerogels: A stable and efficient persulfate activator for the rapid degradation of malachite green. Chemosphere. 251:126402.

Citation: Rathore A, et al. (2023). Azadirachta indica Leaf Mediated Synthesis of Iron Nanoparticles and Their Catalytic Application in Methylene Blue Degradation. Catalysis Research. 3(1):08 .

DOI: https://doi.org/10.35702/catalres.10008